



Thermal Stability Profiling of Co(II), Mn(II), and Ni(II)-Hydrazone Based Complexes: The Role of Kinetic and Thermodynamics Parameters

*¹Iorungwa, M. S., ¹Dafa, S.T., ¹Wuana, R.A., ¹Iornumbe, E. N. and ²Tivkaa, J. T.

¹Inorganic/Physical Chemistry Research Group, Department of Chemistry, Joseph Sarwuan Tarka University
P.M.B. 2373 Makurdi-970001, Nigeria

²Department of Science Laboratory Technology, Benue State Polytechnic, Ugbokolo - Nigeria

*Correspondence Email: iorungwa.moses@uam.edu.ng

ABSTRACT

The thermal stability of the ligands (E)-4-[(2-(2,4-dinitrophenyl)hydrazono)methyl]phenol (**L**₁) and N-(4-hydroxybenzaldehyde)-p-fluoroaniline (**L**₂) along their complexes of Co(II), Mn(II), and Ni(II) were profiled by thermo-gravimetric analysis (TGA), different thermal (kinetic and thermodynamics) parameters viz. Energy of activation (E_a), Entropy of activation (ΔS), Free energy of activation (ΔG), Enthalpy of activation (ΔH) and Frequency factor (A) were calculated using Freeman-Carroll's and Horowitz-Metzger's approximation methods. The thermal results of the ligands showed that they do not contain crystals of water while the complexes contain two molecules of water of hydration. The kinetic parameters revealed that, the decomposition reactions of the synthesized compounds followed first order reaction with the rate constant values ranging from 0.002-0.129 and the activation energies were 55.22, 76.59, 52.90, 52.88 and 75.23 kJmol⁻¹ for (E)-4-[(2-(2,4-dinitrophenyl)hydrazono)methyl]phenol (**L**₁), N-(4-hydroxybenzaldehyde)-p-fluoroaniline (**L**₂), Co(II), Mn(II) and Ni(II) complexes respectively which showed that, **L**₂ and Ni(II) complex requires extra energy to form activated complex as compared to **L**₁, Co(II) and Mn(II) complexes. On the other hand, the frequency factor acquired were 3.56, 5.06, 3.48, 3.50 and 4.97 min⁻¹ for **L**₁, **L**₂, Co(II), Mn(II) and Ni(II) complexes accordingly indicating that, more spaces existed in **L**₂ and Mn(II) complexes than **L**₁, Ni(II) and Co(II) complexes. Thermodynamics parameters results showed that, the Gibb's free energy (ΔG) of the synthesized compounds were positive indicating that, the decomposition was non-spontaneous, The positive values of enthalpy (ΔH) showed that enthalpy is the driving force for the decomposition of the synthesized compounds and exothermic in nature. The negative values of entropy (ΔS) indicate the degree of disorder of the products formed by the dissociations of the bonds is lower than that of the initial reactants.

Keywords: Kinetics, Thermodynamics, [(E)-4-[(2-(2,4-dinitrophenyl)hydrazonomethyl)]phenol, N-(4-hydroxybenzaldehyde)-p-fluoroaniline

INTRODUCTION

Kinetic and thermodynamics profiling of ligands and their complexes is of immense significance and interest since they can provide mechanistic insights into the molecular interactions determining affinity of compounds to its target and are useful to guide the compound selection as well as the subsequent potency enhancement in drug development and discovery (Su and Xu, 2018). The breakdown of the bonds in the metal complexes provides a means of evaluating the stability of the complexes formed by different metal ions and ligands (Linkuviene *et al.*, 2018; Malacaria *et al.*, 2021). Kinetic and thermodynamics profiling of ligands and their complexes is useful for the preparation of metal complexes possessing pores, lattice defect and therefore they act as reactive solids (Sodhi and Paul, 2019) and they also provide information about the balance of energetic forces driving binding interactions and is essential for understanding and optimizing molecular interactions (Garbett and Chaire, 2012). Thermal

behaviour of ligands and their complexes is one of the most convenient measures of their reactivity and pre-treatment studied at selected isothermal temperatures, which can modify the properties of the ligands and their complexes in an important way by creating imperfections and effect on kinetics of decomposition (Papadopoulos *et al.*, 2015; Cylkowska *et al.*, 2020). The ligands and their complexes may result in the modification of their thermal behavior, geometry and electronic properties which lead to changes in their biological functions (Rodica *et al.*, 2010; Masoud *et al.*, 2022). It is found that many workers studied thermal decomposition of ligands and their complexes preparing them by different techniques (Masoud *et al.*, 2018; Elemo *et al.*, 2019; Ikram *et al.*, 2020). The objective of this work is to profile the kinetic and thermodynamics parameters which Co(II), Mn(II), and Ni(II)-Hydrazones based complexes on thermal decomposition. So far, no report on the thermal decomposition of Co(II), Mn(II), and Ni(II)-Hydrazones based complexes

has been documented. Non-isothermal thermogravimetric analysis (TGA) has been widely used as a tool to investigate the thermal stability of complexes (Gola *et al.*, 2023). Thermograms obtained, provide the information about the sample composition, thermal stability as well as the kinetic data relating the chemical changes that occur on heating (Sarsensenbekova *et al.*, 2023).

MATERIALS AND METHODS

All the chemicals and solvents used for the thermo-gravimetric analysis were of analytical grade and purchased from JDP Chemicals. They were used without additional purification.

Thermo-gravimetric Analysis (TGA) of Co(II), Mn(II), and Ni(II)-Hydrazone Based Complexes

The TGA of Co(II), Mn(II), and Ni(II)-Hydrazones based complexes was carried using the method described by Zaware and Jadhav, (2015) with modifications. The ligands and metal complexes were analyzed using UW-MSE TA Instruments TGA Q50 thermal analyzer at heating rate of 5 °C/min and in air (Nitrogen) atmosphere up to 650 °C. A small sample of about 15 mg was loaded into the ceramic crucible in order to avoid the effect of mass and heat transfer limitation. The atmosphere nitrogen was continuously flowed into the inner part of the heating chamber during the thermal degradation process. The sample was subjected into the pre-adjusted heating program from room temperature till to 650°C. The respective TGA data were resulted during the experiment and the thermograms were recorded which revealed changes in the structure and other important properties of ligands and metal(II)-hydrazone based complexes being studied as shown in Figure (1-5).

Thermal stability profiling of ligands along their complexes of Co(II), Mn(II), and Ni(II)

The kinetics of degradation of ligands and Co(II), Mn(II) and Ni(II) complexes was examined as a first-order reaction for the purpose of simplification (Klippensteine *et al.*, 2014; Vafazadeh and Bagheri, 2015; Stroberg and Schned, 2017) in the analysis. The kinetic profiling of the individual ligands with their complexes was carried out by tracing the following selected temperature viz: 150, 200, 250, and 300 °C to the percentage mass loss axis and the masses lost were obtained from which representative graphs for Freeman-Carroll (Figure 6) and Horowitz-Metzger (Figure 7) methods were plotted to evaluate the basic kinetic parameters of the decomposition reaction viz: activation energy (E_a), frequency factor (A), order of reaction (n), and the rate constant (k). The activation energy (E_a) of the ligands and their complexes was calculated from the slope ($-E_a/2.303R$) of Freeman-Carroll plot (Figure 6) while for Horowitz-Metzger (Figure 7),

the activation energy was determined from the slope ($E_a/2.303RT_s^2$) (Gul *et al.*, 2018; Chaudhary *et al.*, 2019).

RESULTS AND DISCUSSION

Thermogravimetric analysis of ligands **1** and **2** alongside their complexes were performed at 5 °C/min and the decomposition patterns with thermo-gravimetric (TGA) curve are shown in Figure 1-5 with the intent of suggesting the existence of lattice/coordinated (water) and at the same time profile the kinetic and thermodynamic parameters of the ligands with their complexes. The thermogram represents the relationship between changes in mass on the temperature which gives information about the nature of the TG curves and percent weight losses at various temperatures.

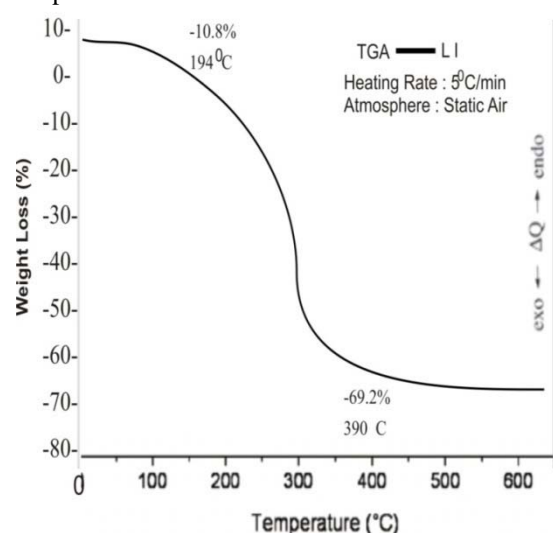


Figure 1: Thermogram of Ligand 1(L1)

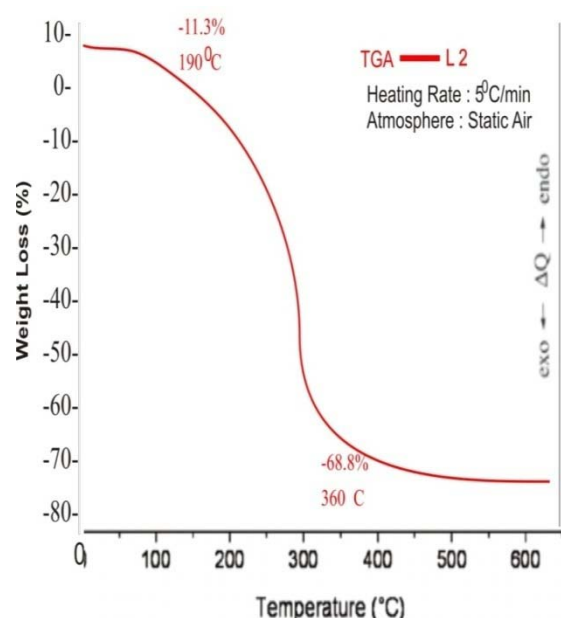


Figure 2: Thermogram of Ligand 2 (L2)

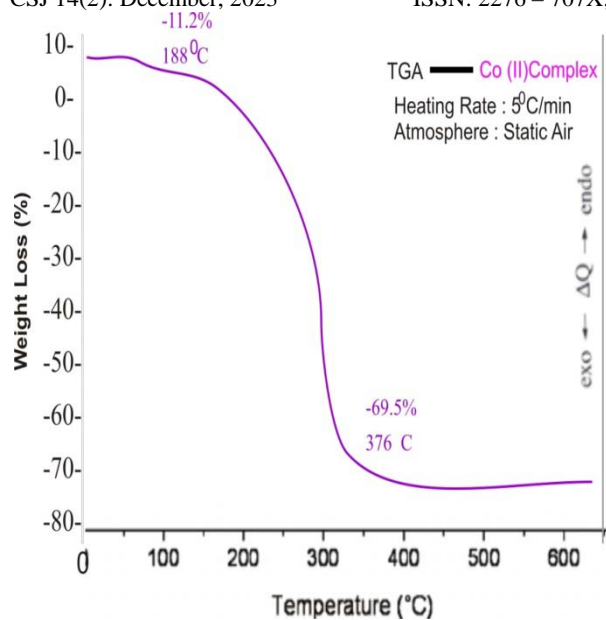


Figure 3: Thermogram of Co(II) Complex

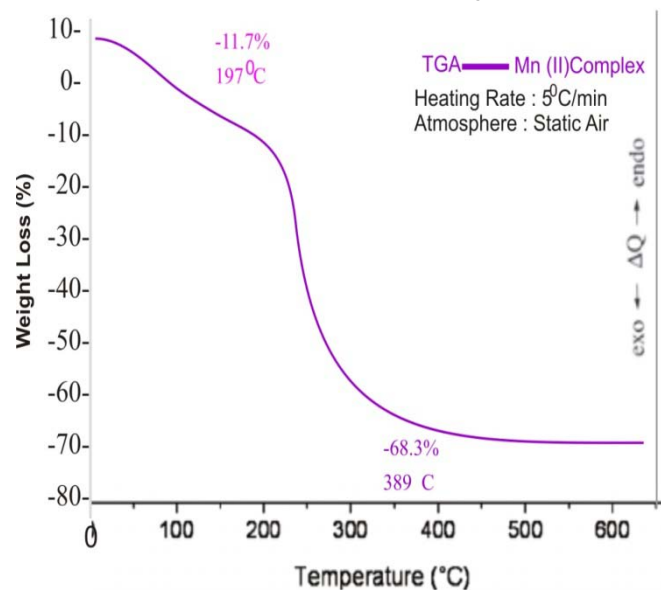


Figure 4: Thermogram of Mn(II) Complex

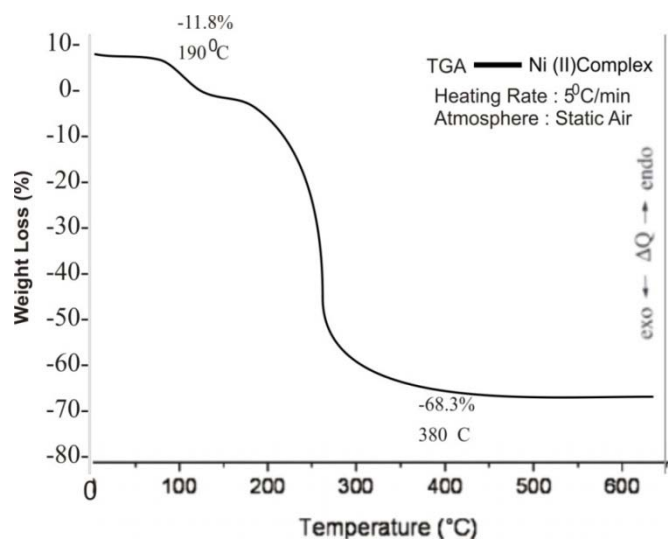


Figure 5: Thermogram of Ni(II) Complex

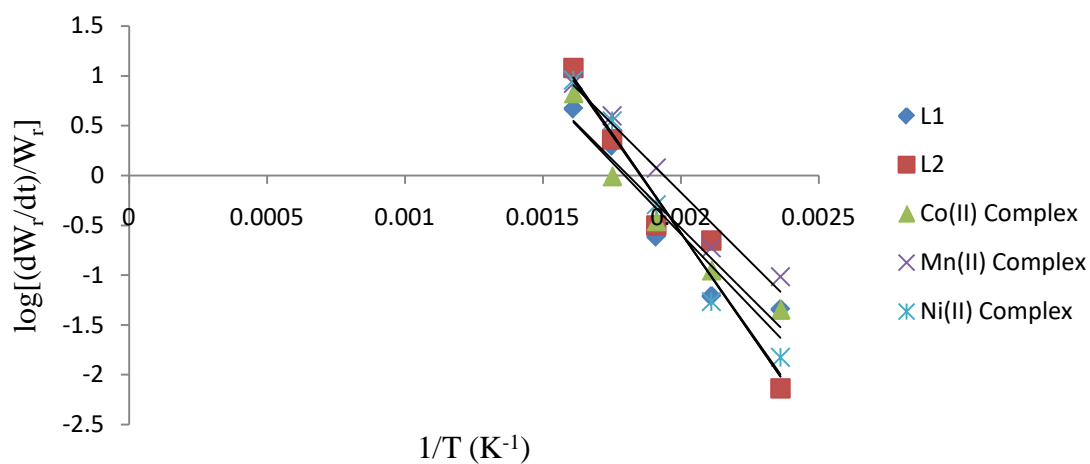


Figure 6: Freeman-Carroll plot of L_1 , L_2 , Co(II), Mn(II) and Ni(II) Complexes for the calculation of Activation Energy (E_a) and Pre-exponential factor (A)

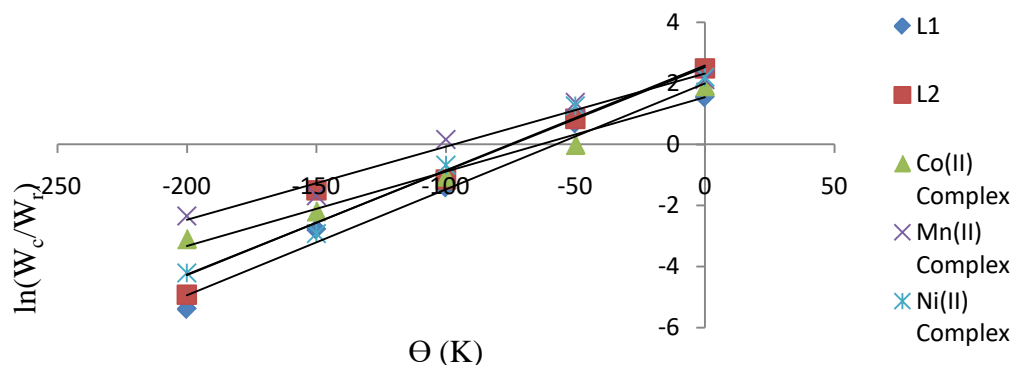


Figure 7: Horowitz-Metzger plot of L_1 , L_2 , Co(II), Mn(II) and Ni(II) Complexes for the calculation of Activation Energy (E_a) and Pre-exponential factor (A)

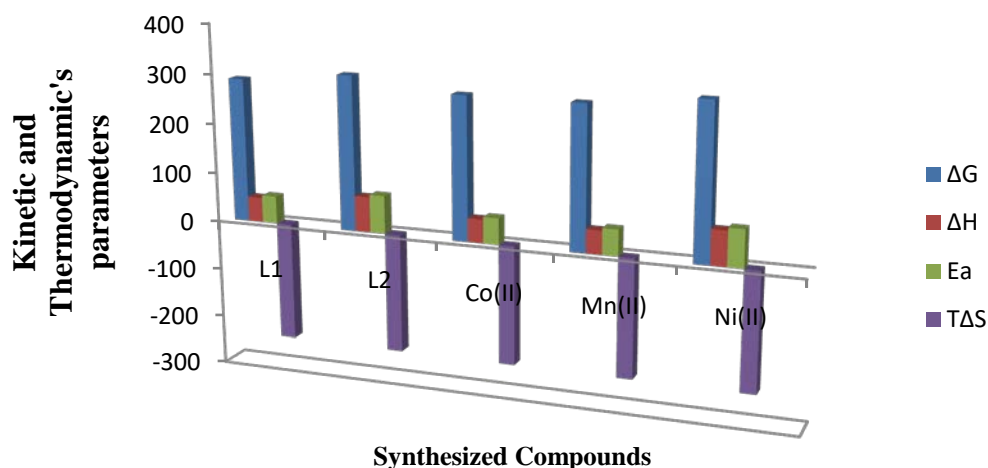


Figure 8: Comparison of Gibb's free energy (ΔG), Enthalpy (ΔH), Activation energy (E_a) and Entropy ($T\Delta S$) of ligands, and Metal Complexes using Freeman-Carroll methods to depict the relationship between stability and activation energy.

Table 1: Thermoanalytical data and Decomposition Temperature for Ligands and Complexes

Compounds	Decomposition Steps	Temperature Range ($^{\circ}\text{C}$)	Species Degraded	Weight Loss (%)	
				Found	Cal.
L_1	1	60-194	-OH and two $-\text{NO}_2$	10.8	
	2	194-390	Two side benzene rings along with $(-\text{CH}_2)$ groups	69.2	
L_2	1	67-190	-OH and $-\text{F}$	11.3	
	2	190-360	Two side benzene rings along with $(-\text{CH}_2)$ groups	68.8	
Co(II) Complex	1	61-149	Two H_2O molecule	11.2	
	2	149-188	-OH, $-\text{F}$ and two $-\text{NO}_2$	14.1	
	3	188-376	Four side benzene rings along with $(-\text{CH}_2)$ groups	69.5	
Mn(II) Complex	1	22-100	Two H_2O molecule	03.0	
	2	100-197	-OH, $-\text{F}$ and two $-\text{NO}_2$	11.7	
	3	197-389	Two side benzene rings along with $(-\text{CH}_2)$ groups	68.3	
Ni(II) Complex	1	85-150	Two H_2O molecule	04.0	
	2	150-190	-OH, $-\text{F}$ and two $-\text{NO}_2$	11.8	
	3	190-380	Two side benzene rings along with $(-\text{CH}_2)$ groups	68.3	

Table 2: Rate of Change of Weight with Temperature obtained from TGA of Ligands and Complexes in Nitrogen for Freeman-Carroll Method

Compounds	(dw/dt)	w_r	$(dw_r/dt)/w_r$	T (K)	$\frac{1}{T}$ (K ⁻¹)	$\log \left[\frac{(dw_r/dt)}{w_r} \right]$
L₁	03.00	66.20	0.0453	423	0.00236	-1.344
	04.00	65.20	0.0614	473	0.00211	-1.212
	13.50	55.70	0.2424	523	0.00191	-0.616
	46.00	23.20	1.9828	573	0.00175	0.297
	57.00	12.20	4.6721	623	0.00161	0.670
L₂	0.50	68.30	0.0073	423	0.00236	-2.137
	12.50	56.30	0.2220	473	0.00211	-0.654
	16.50	52.30	0.3155	523	0.00191	-0.501
	48.00	20.80	2.3077	573	0.00175	0.363
	63.50	05.30	11.9811	623	0.00161	1.079
Co(II)	03.00	66.50	0.0451	423	0.00236	-1.346
	07.00	62.50	0.1120	473	0.00211	-0.951
	18.00	51.50	0.3495	523	0.00191	-0.457
	34.50	35.00	0.9857	573	0.00175	-0.006
	60.50	09.00	6.7222	623	0.00161	0.828
Mn(II)	06.00	62.30	0.0963	423	0.00236	-1.016
	10.75	57.55	0.1868	473	0.00211	-0.729
	37.00	31.30	1.1821	523	0.00191	0.073
	54.50	13.80	3.9493	573	0.00175	0.597
	61.00	07.30	8.3562	623	0.00161	0.922
Ni(II)	01.00	67.30	0.0149	423	0.00236	-1.827
	3.50	64.80	0.0540	473	0.00211	-1.268
	23.00	45.30	0.5077	523	0.00191	-0.294
	53.25	15.05	3.5382	573	0.00175	0.549
	61.50	06.80	9.0441	623	0.00161	0.956

Key: dw/dt = rate of change of weight with time. $w_r = W_c - W$ W_c = weight loss at completion of reaction.
 W = fraction of weight loss at a particular temperature.

Table 3: Rate of Change of Weight with Temperature obtained from TGA of Ligands and Complexes in Nitrogen for Horowitz –Metzger Method

Compounds	W_c	w_r	W_c/w_r	T (K)	θ	$\ln \left(\frac{W_c}{w_r} \right)$
L₁	03.00	66.20	0.0453	423	-200	-5.3970
	04.00	65.20	0.0614	473	-150	-2.7904
	13.50	55.70	0.2424	523	-100	-1.4172
	46.00	23.20	1.9828	573	-50	0.6845
	57.00	12.20	4.6721	623	0.00	1.5416
L₂	0.50	68.30	0.0073	423	-200	-4.9199
	12.50	56.30	0.2220	473	-150	-1.5051
	16.50	52.30	0.3155	523	-100	-1.1534
	48.00	20.80	2.3077	573	-50	0.8363
	63.50	05.30	11.9811	623	0.00	2.4833
Co(II)	03.00	66.50	0.0451	423	-200	-3.0989
	07.00	62.50	0.1120	473	-150	-2.1893
	18.00	51.50	0.3495	523	-100	-1.0513
	34.50	35.00	0.9857	573	-50	-0.0144
	60.50	09.00	6.7222	623	0.00	1.9054
Mn(II)	06.00	62.30	0.0963	423	-200	-2.3403
	10.75	57.55	0.1868	473	-150	-1.6777
	37.00	31.30	1.1821	523	-100	0.1673
	54.50	13.80	3.9493	573	-50	1.3735
	61.00	07.30	8.3562	623	0.00	2.1230
Ni(II)	01.00	67.30	0.0149	423	-200	-4.2064
	3.50	64.80	0.0540	473	-150	-2.9188
	23.00	45.30	0.5077	523	-100	-0.6779
	53.25	15.05	3.5382	573	-50	1.2636
	61.50	06.80	9.0441	623	0.00	2.2021

Table 4: Kinetic Activation Parameters for Non-isothermal Ligands along Complexes by TGA in Air using Freeman-Carrol Method

Compounds	Trendline equation	R ²	Kinetics Parameters			
			E _a (kJ/mol)	A × 10 ³ (min ⁻¹)	Reaction Order (n)	Rate constant (k)
L ₁	-2884x + 5.177	0.906	55.22	3.65	0.71	0.086
L ₂	-4000x + 7.422	0.959	76.59	5.06	0.87	0.002
Co(II) Complex	-2763x + 4.996	0.936	52.90	3.48	0.70	0.128
Mn(II) Complex	-2762x + 5.350	0.966	52.88	3.50	0.73	0.129
Ni(II) Complex	-3929x + 7.277	0.978	75.23	4.97	0.86	0.003

Key: E_a = Activation energy, n = Order of reaction and A = pre-exponential factor

Table 5: Kinetic Activation Parameters for Non-isothermal Ligands along Complexes by TGA in Air using Horowitz-Metzger Method

Compounds	Trendline equation	R ²	Kinetics Parameters			
			E _a (kJ/mol)	A × 10 ⁴ (min ⁻¹)	Reaction Order (n)	Rate constant (k)
L ₁	0.0081x + 1.99	0.975	60.45	1.50	0.69	0.128
L ₂	0.0099x + 2.53	0.947	73.40	5.15	0.93	0.036
Co(II) Complex	0.0078x + 1.55	0.978	58.13	3.78	0.44	0.505
Mn(II) Complex	0.0075x + 2.32	0.984	56.88	5.52	0.94	0.929
Ni(II) Complex	0.0105x + 2.56	0.976	79.67	2.26	0.84	0.005

Table 6: Thermodynamics Parameters for Non-isothermal Ligands along Complexes by TGA in Air using Freeman-Carrol Method

Compounds	ΔH (kJmol ⁻¹)	ΔG (kJmol ⁻¹)	ΔS (Jmol ⁻¹)	β
L ₁	50.04	288.42	-0.383	-1.057
L ₂	71.41	309.79	-0.383	-1.061
Co(II) Complex	47.72	286.10	-0.383	-1.056
Mn(II) Complex	47.70	286.08	-0.383	-1.056
Ni(II) Complex	70.05	308.43	-0.383	-1.061

Thermal decomposition results of the ligands and their Co(II), Mn(II) and Ni(II) complexes

Thermal decomposition is a chemical decomposition caused by heat. The decomposition temperature of the ligands and their complexes is the temperature at which the ligands and their complexes decompose.

The thermograms of the L₁ and L₂ are presented in Figure 1 and 2. The two thermograms demonstrate a continuous weight loss signifying decomposition by fragmentation with increase in temperature (Burkanudeen *et al.*, 2016). A cautious analysis of the thermogram of the two ligands shows that, the decomposition occurred in two steps which imply that, the two ligands did not contain water molecules (lattice/crystal) due to decomposition (Grivel, 2014). L₁ is stable up to 60 °C while L₂ is stable up to 67 °C. The slight difference in their stability could be attributed to the differences in the functional groups attached to the ligands (Ni *et al.*, 2014). The thermogram of L₁ showed the first step slow decomposition between 60 to 194 °C corresponding to 10.8 % loss which

may be attributed to (-OH) and two (-NO₂) groups linked with ligand (Lyu *et al.*, 2021) while the thermogram of L₂ showed the first step slow decomposition between 67 to 190 °C corresponds to 11.3 % loss which may be attributed to (-OH) and -F groups linked with ligand. A significant difference in the initial decomposition temperature and mass loss behaviour of the two ligands is apparently due to the branched chain and the crystalline nature of the two ligands under the condition of interface conversion of higher molecular compound to lower one (Andrianova *et al.*, 2020). The second step of decomposition starts from 194-390 °C for L₁ which represents the degradation of two side benzene rings along with (-CH₂) which correspond to 69.2 % while the thermogram of L₂ showed and the second step decomposition from 190- 360 °C corresponding to 68.8 % loss of two side benzene rings along with -CH₂ groups. The thermal degradation by increasing temperature may be due to the increasing strain, instability and cross linking of molecule by increasing thermal vibration. To decrease the strain

and to maintain stability, the ligands and complexes undergoes degradation. The synthesized ligands and complexes were half decomposed at 210 °C observed from thermal data. The decomposition is due to pyrolysis of straight chain linked structure of ligands and at 390 °C, degradation process occurs up to final level leaving behind the remaining moieties.

The thermogram of the Co(II), Mn(II), and Ni(II) complexes represented in Figure 3-5 shows that, their thermal decomposition occurred in three steps indicating that, the complexes contains water molecules. The gradual weight loss due to loss of water molecules is observed in the temperature range of 22-85 °C which demonstrate that, the water molecules eliminated from the complexes were crystal (lattice) water (Ahamed *et al.*, 2014). According to Nikolaev *et al.* (1969), water eliminated below 150 °C can be considered as lattice or crystal water and the one eliminated above 150 °C may be due to coordination to the metal ion. The TG curves indicate that above 149 °C, the dehydrated product of Co(II) complex start to loss mass with partial evaporation of the ligand which corresponds to 14.1 % while Mn(II) dehydrated product begins losing mass at 100 °C which was 11.7 % and dehydrated Ni(II) complexes losses 11.8 % at the beginning which correspond to a temperature of 150 °C. In the final temperature range of 188-389°C, all the ligands of the three complexes were lost and the final products are metal oxides (Li and Zhong, 2014).

$$Ze^{-E_a/RT} = \left(\frac{-dx/dt}{x^n} \right)$$

The logarithmic form of equation (1) is differentiated with respect to $\frac{dt}{dx}$, x and T to get

$$E_a \frac{dt}{RT^2} = d \ln \left[\frac{-dx/dt}{x^n} \right] - n d \ln x \quad (2)$$

Integrating equation (2) and rearranging

$$E_a \frac{dt}{RdT^2} \ln x = \left[\frac{d \ln [-dx/dt]}{d \ln x} \right] - n \quad (3)$$

$$\left[\frac{-E_a/R}{\Delta(1/T)} \right] \Delta \ln x = \left[\frac{d \ln [-dx/dt]}{d \ln x} \right] - n \quad (\text{Sharma } et al., 2017) \quad (4)$$

This may be written in the form

$$\log \left[\frac{dw/dt}{w_r} \right] = -E_a/2.303R(1/T) + \log Z \quad (\text{Zaware and Jadhav, 2015}) \quad (5)$$

Where w = mass loss, $w_r = w_c - w$, w_c = maximum mass loss. It follows from Equation (2) that a plot of $[(dw/dt)/w_r]$ against $(1/T)$ gives a straight line with a slope equal to $-E_a/2.303R$ and

$$\ln \left[1 - \frac{(1-\alpha)^{1-n}}{n-1} \right] = \ln \left[\frac{zRT_s^2}{\phi E_a} \right] - \frac{E_a}{RT_s} + \frac{\theta E_a}{RT_m^2} \quad \text{for } n \neq 1 \quad (6)$$

$$\ln \ln \left(\frac{W_\infty}{W_r} \right) = \frac{E_a \theta}{RT_m^2} \quad \text{for } n = 1 \quad (7)$$

$$\text{where } \theta = T - T_m \quad (8)$$

A plot of $\ln \left(\frac{W_\infty}{W_r} \right)$ versus θ will give a straight line, the slope of which is equal to $E_a/2.303RT_s^2$ from which E and A can be calculated by taking $R = 8.314 \text{ J} \cdot \text{mol}^{-1} \cdot \text{K}^{-1}$, $\beta = 5^\circ\text{C} \cdot \text{min}^{-1}$ (Kulkarni *et al.*, 2019).

$$A = \frac{E_a}{RT_m^2} \beta \exp \left(\frac{E_a}{RT_m} \right) \quad (9)$$

where E_a = activation energy from graph

Thermal kinetic and thermodynamics profiling of the ligands and their Co(II), Mn(II) and Ni(II) complexes

Thermograms of ligands alongside their complexes are shown in Figure 1-5. An examination of thermograms showed two decomposition steps while their complexes depicted three decomposition steps in the temperature range 0 °C to 650 °C. The differences in the number of steps of decomposition of ligands and their complexes confirmed the complexation of the ligands and metal salts as suggested by the electronic spectra. It is also detected that all the thermograms of the ligands and their complexes were curved indicating that, the decomposition reactions followed first order kinetics with the gradient of the curves in the order of $L_2 < \text{Ni(II) complex} < L_1 \text{ Co(II) complex} < \text{Mn(II) complex}$ suggesting the speed of the decomposition which could be attributed to the number of electron releasing (-OH, -NR₂) or withdrawing groups (-F, -NO₂) which increased or lowered the electron density at the reactive centers hence increases or decreases the thermal stability (Elemo *et al.*, 2019; Andrianova *et al.*, 2020).

Ligands and complexes underwent thermal degradation during the experiment and their reaction rate was represented by the following equation:

Freeman-Carroll differential method (Zaware and Jadhav, 2015) in 1958 was developed (1) by differential method.

intercept equal to $\log Z$ (Tonbul and Yurdakoc, 2001).

Hugh H. Horowitz and Gershon Metzger in 1962 derive an Equation

The kinetic parameters obtained using Freeman-Carroll and Horowitz-Metzger plots are presented in Tables 4 and 5 respectively which were observed to be in conformity and hence the parameters obtained via Freeman-Carroll plot were selected for discussion in this work. The values of activation energy (E_a) obtained were 55.22, 76.59, 52.90, 52.88 and 75.23 kJoules for L_1 , L_2 , Co(II), Mn(II), and Ni(II) complex respectively which were positive relatively small values activation energy (E_a) demonstrating that the rate of the decomposition increased with increasing temperature and the “apparent” rate constant of the overall decomposition defined by Arrhenius behaviour will increase as temperature was increased which is a signal that the decomposition of the ligands alongside their complexes had no complex mechanism (Iorungwa *et al.*, 2019) and the relatively higher values of activation energy of L_2 and Ni(II) complex explained the extra energy needed by L_2 and Ni(II) complex as compared to L_1 , Co(II) and Mn(II) complex to undergo decomposition which was confirmed by small mass loss by L_2 and Ni(II) complex as shown in Table 6 signifying that a higher activation energy prevented the formation of activated complex (Piskulich *et al.*, 2019). The values of E_a of the ligands and their complexes are in the order of Mn(II) < Co(II) complex < L_1 < Ni(II) < L_2 . The difference in the values of E_a (Activation energy) of the ligands was due to the differences in the nature of chemical bonds (Dafa, 2023) while for the complexes was because of the decrease in their ionic radius as the smaller size of ions allowed a closer approach of ligands (Al-Awadi *et al.*, 2008). Therefore, for isostructural M(II) complexes, the E_a values were found to increase in the order of Mn < Co < Ni.

The frequency factor (A) can be visualized as the frequency of correctly oriented collisions

$$\Delta H = E_a - RT \quad (\text{Singh } et al., 2020) \quad (10)$$

Gibbs Free Energy

Gibbs free energy is also known as free enthalpy, and it represents the total increase in energy of the system for the formation of the

$$\Delta G = E_a + RT_m \times \ln \left(\frac{K_B \times T_m}{h \times A} \right) \quad (\text{Palmy } et al., 2021) \quad (11)$$

where ΔG is the Gibbs free energy; A = frequency factor, (min^{-1}); K_B = Boltzmann constant (1.38×10^{-23} J/K); E_a = activation energy (kJ/mol); h = Planks constant (Js); R = universal gas constant ($\text{kJ}^{-1} \cdot \text{mol}^{-1}$) and T_m = temperature of maximum decomposition in (K).

$$\Delta S = \frac{\Delta H - \Delta G}{T_m} \quad (\text{Valapa } et al., 2014) \quad (12)$$

Where ΔG = change in internal energy (kJ/mol); ΔH = enthalpy change (kJ/mol); T_m = Temperature of maximum decomposition in (K) and ΔS = entropy change

between reactant particles (Sbirrazzouli, 2020). The frequency factor (logA) values can be used to predict space or volume in the reacting molecules (Vyazovkin, 2021). The A obtained in this study were 3.56, 5.06, 3.48, 3.50, and 4.97 for L_1 , L_2 , Co(II), Mn(II), and Ni(II) complex in that order. The values demonstrate that, the frequency of collisions in L_2 and Mn(II) complex was more than the frequency of collision in L_1 , Co(II) and Ni(II) complex due to spaces or volume in between the reacting molecules (Al-Moameri *et al.*, 2017; Wang *et al.*, 2018). In theory, with decreasing the value of E_a , the value of logA increased and elevated value of E_a indicates higher stability. Nevertheless, there lie some inbuilt physical and chemical factors which may cause a departure from this trend. Higher value of E_a and lower value of A favours the reaction to proceed slower than normal (Triyono, 2010; Bartocci *et al.*, 2019; Wang *et al.*, 2021). The decomposition reaction of the ligands and the complexes, judging from the R^2 values followed the first order reaction (n) with R^2 values closed to unity while the values of the rate constant (k) obtained showed that as activation energy increase, the rate constant decreases and therefore the rate of reaction decreases as can be seen in Table 4 and 5.

The thermodynamics parameters of the thermal decomposition of the ligands and their complexes viz: the enthalpy (ΔH), the Gibbs free energy (ΔG) and the entropy change (ΔS) were obtained from Freeman-Carroll plot by using equations: 10, 11 and 12 are presented in Table 4.

Enthalpy

The enthalpy of the thermal decomposition in this study was obtained by using Equation (10):

activated complex and was obtained from the following Equation (11) to determine the feasibility and spontaneity of the thermal degradation process.

Entropy

The entropy which is thermodynamics parameter that indicates the degree of disorder of the ligands and their complexes was determined in this study via the equation (12):

The enthalpy is the thermodynamic property that represents the total heat content of a system at constant pressure when the only work done is pressure-volume. For this study, enthalpy means the total energy consumed by the ligands

and their complexes for their conversion into various products (Singh *et al.*, 2020). The enthalpy (ΔH) for ligands and their complexes in this study were 50.04, 71.41, 47.72, 47.70 and 70.05 kJ mol^{-1} for L_1 , L_2 , Co(II), Mn(II), and Ni(II) complex respectively and were all observed to be positive which showed that for decomposition reaction, energy was absorbed during the reaction i.e endothermic (Ohia *et al.*, 2013). The enthalpy of L_2 was found to be greater than L_1 . This implies that, the total energy consumed by L_2 to be splitted into the various components parts was more than the energy consumed by L_1 this could be due to the extra stability of L_2 which could be as a result of the increasing strength of hydrogen bonding which is in the Oder of $S < Cl < N < O < F$. The more electronegative the element, the higher the chances of hydrogen bonding (Housecroft and Sharpe, 2005) and the more the energy needed to break the chemical bond present in the individual ligands (Batsanov, 2022). The stability of complexes increased with decrease in the size of the metal ion. For M(II) ions, the general trend in stability for complexes known as Irving-Williams series $Mn(II) < Co(II) < Ni(II)$.

Gibbs free energy is also known as free enthalpy, and it represents the total increase in energy of the system for the formation of the activated complex (radical formation from the ligands and their complexes) (Palmy *et al.*, 2021) and is obtained in this study from Equation (12). The Gibbs free energy (ΔG) values were 288.42, 309.79, 286.10, 286.08 and 308.43 kJ mol^{-1} for L_1 , L_2 , Co(II), Mn(II), and Ni(II) complex respectively and were all viewed to be positive. The positive values of the Gibbs free energies indicated that the process requires a contribution of energy for it to occur (non-spontaneous process), taking into account that ΔG means a total increase in the energy of the system for the formation of the activated complex (Kim *et al.*, 2010). On the contrary, the values of entropies for both ligands and complexes were found to be -0.383 kJoule for all the ligands and their complexes. The negative values of entropies, indicates that the degree of disorder of the products formed through dissociation of bonds is lower than that of the reactants. The low ΔS at the rate of 5 $^{\circ}\text{C} / \text{min}$ means that the ligands and complexes only underwent some physical and chemical changes, until it reached a state close to its thermodynamic equilibrium. Ligands and complexes have little reactivity and it took a long time to form an activated complex. Moreover, a high ΔS means that the reactivity will be high, and it will take less time to form the activated complex; this happens when the heating rate is lower (Kennedy and Hodzic, 2021).

The values for overall stability ($\log\beta$) were -1.057, -1.061, -1.056, -1.056 and -1.061 for L_1 , L_2 , Co(II), Mn(II) and Ni(II) complexes respectively. The negative overall stability

indicated the decomposition stability of the ligands and their complexes with L_2 and Ni(II) complex having overall decomposition stability which was lower than L_1 , Co(II) and Mn(II) complexes demonstrating that, L_2 and Ni(II) complex were in a reduced amount of decomposition reactivity than L_1 , Co(II) and Mn(II) complexes (Sukarni *et al.*, 2018). This result concured with the higher activation energy (76.59 and 75.23 KJ/mol) and the lower rate constant (0.002 and 0.003) of L_2 and Ni(II) complex as compared to higher activation energy (55.22, 52.90 and 52.88 KJ/mol) and rate constant (0.086, 0.128 and 0.129) of L_1 , Co(II) and Mn(II) complexes indicating the strength of hydrogen bond in the individual ligands and the binding strength of the ligands and metal ions (Geoffrey, 2010).

Comparison of the Kinetic Parameters with Structure and Thermal Stability

The activation energies (E_a) of the ligands and the complexes vary in the range 55.75 to 78.23 $\text{kJ}\cdot\text{mol}^{-1}$. The corresponding values of pre-exponential factor (A) of these complexes come in the range 3.09 to 4.92 min^{-1} while the respective values of Gibb's free energy entropy of ligands and their complexes fall in the range 286.08 to 309.79 kJ mol^{-1} and the entropy of activation (ΔS) for both ligands and their complexes was -0.383 $\text{J}\cdot\text{mol}^{-1}$.

Based on the activation energies obtained from the thermal decomposition of the ligands and their complexes; L_2 and Ni(II) complex were found to be highly stable respectively, while Mn(II) complex was found to be least stable. The negative value of the entropy of activation also indicates that the activated complexes are more ordered than reactants. Even though there is common entropy of activation (ΔS) present in all the ligands and their complexes, there is a variation in the different kinetic parameters. This variation could be due to the effect of structure (Nature of bonds and group of atoms present in the structure) on the thermal decomposition of the complexes. Hence, the structures play an important role on the thermal decomposition kinetic and thermodynamics parameters of the ligands and their complexes (Elemo *et al.*, 2019).

CONCLUSION

Thermal stability (kinetic and thermodynamics) profiling of ligands L_1 , L_2 and their metal complexes of Co(II), Mn(II) and Ni(II) were carried out. The kinetic profiling results revealed that, the decomposition reactions of the ligands and their complexes followed first order reaction and the activation energy obtained showed that, L_2 and Ni(II) complex requires extra energy to form activated complex as compared to L_1 , Co(II) and Mn(II) complexes. Meanwhile, the results of frequency factor showed that, more spaces or volume could exist in L_2 and Mn(II) complexes than L_1 , Ni(II) and Co(II) complexes.

Thermodynamics parameters results of the study showed that, the Gibb's free energy (ΔG) of the ligands their complexes were positive indicating that, the process required a contribution of energy for it to occur (non-spontaneous process), taking into account that ΔG means a total increase in the energy of the system for the formation of the activated complex. The obtained positive values of enthalpy (ΔH) showed that enthalpy is the driving force for the decomposition of the ligands and their complexes. However, the negative values of entropy (ΔS) indicate the degree of disorder of the products formed by the dissociations of the bonds is lower than that of the initial reactants (ligands and their complexes). Furthermore, an extremely low entropy value shows that only certain physical and chemical changes occur in the ligands and their complexes. Consequently, if the enthalpy is low, the entropy must have a high negative value to favor the reaction. This indicates that the evolution of the reaction will not only depend on energy (enthalpy), since it will also depend on the molecular configuration that is reached (changes in entropy).

REFERENCES

- Ahamed, M. A. R., Azarudeen, R. S. and Kani, N. M. (2014). Antimicrobial applications of transition metal complexes of benzothiazole based terpolymer: Synthesis, characterization, and effect on bacterial and fungal strains. *Bioinorganic Chemistry and Application*, 10: 1-16.
- Al-Moameri, H., Jaf, L. and Suppes, G. J. (2017). Viscosity-dependent frequency factor for modelling polymerization kinetic. *RSC Advances*, 7:26583-26592.
- Al-Moameri, H., Jaf, L. and Suppes, G. J. (2017). Viscosity-dependent frequency factor for modelling polymerization kinetic. *RSC Advances*, 7:26583-26592.
- Andriianova, A. N., Biglova, Y. N. and Mustaffin, A. G. (2020). Effect of structural factors on the physicochemical properties of functionalized polyanilines. *RSC Advances*, 10 (13): 7468-7491.
- Bartocci, P., Tschentscher, R., Stensrød, R. E., Barbanera, M. and Fantozzi, F. (2019). Kinetic analysis of digestate slow pyrolysis with the application of the master-plots method and indepent parallel reactions scheme, *Molecules*, 24 (9): 1657.
- Batsanov, S. S. (2022). Energy electronegativity and chemical bonding. *Molecules*, 27(23): 8215-8220.
- Burkanudeen, A. R., Ahamed, M.A., Azarudeen, R. S., Begum, M. S. and Gurnule, W. B. (2016). Thermal degradation kinetics and antimicrobial studies of terpolymer resins. *Arabian Journal of Chemistry*, 9: 296-305.
- Chaudhary, R. G., Ali, P., Gandhare, N. V., Tanna, J. A. and Juneja, H. D. (2019). Thermal decomposition kinetics of some transition metal coordination polymers of fumaroyl bis(paramethoxyphenylcarbamide) using DTG/DTA techniques. *Arabian Journal of Chemistry*, 12 (7):1070-1082.
- Cylkowska, A., Rogalewicz, B., Raducka, A., Blaszczyk, N., Maniecki, T., Wieczorek, K. and Mierczyński, P. (2020). Synthesis, spectroscopic, thermal and catalytic properties of four new metal(II) complexes with selected N- and O-donor ligands. *Materials (Basel)*, 13 (14): 3217-3225.
- Dafa, S. T. (2023); Co(II), Mn(II), and Ni(II)-hydrazone based complexes: grinding as a solvent-free synthesis, characterization, thermal profiling and antimalaria studies. Ph.D. Thesis, Department of Chemistry, Joseph Sarwuan Tarkaa University, Makurdi, Nigeria. Pp 1 – 150.
- Elemo, F., Gebretsadik, T., Gebrezgiabher, M., Bayeh, Y. and Thomas, M. (2019). Kinetics on Thermal Decomposition of Iron(III) Complexes of 1,2-Bis(Imino-4'-Antipyrinyl)Ethane with Varying Counter Anions. *Advances in Chemical Engineering and Science*, 9: 1-10.
- Garbett, N. C. and Chaire, J. B. (2012). Thermodynamic studies for drug design and screening. *Expert Opinion Drug Discovery*, 7(4): 299-314.
- Geoffrey, A. L. (2010). Introduction to coordination chemistry. John Wiley and Sons, Ltd., Publication, Pp 83-170.
- Gola, A., Knysak, T., Mucha, I. and Musial, V. (2023). Synthesis, thermogravimetric analysis, and kinetic study of poly-N-isopropylacrylamide with varied initiator content. *Polymer*, 15(11): 2427-2430.
- Grivel, J. (2014). Thermal decomposition of RE(C₂H₅CO₂)₃ center dot H₂O (RE = Dy, Tb, Gd, Eu and Sm). *Journal of Thermal Analysis and Calorimetry*, 115 (2): 3467
- Gul, H., Alisha, A-H., Bilal, S. and Gul, S. (2018). Study on the thermal decomposition kinetics and calculation of activation energy of degradation of poly(*o*-toluidine) using thermogravimetric analysis. *Iranian Journal of Chemistry & Chemical Engineering*, 37(1): 83-88
- Housecroft, C. E. and Sharpe, A. G. (2005). Inorganic chemistry, 2nd edition, Pearson Prentice-Hall, Pp 20-21.
- Ikram, M., Rehman, S., Ayaz, M. and Salman, S. M. (2020). Synthesis, spectral, thermal and DPPH scavenging studies of the hydrazone derived transition metal complexes. *Journal of Chemical Society of Pakistan*, 42 (6): 888-889.

- Iorungwa, M. S., Wuana, R. A., Dafa, S. T. (2019). Synthesis, Characterization, Kinetics, Thermodynamic and Antimicrobial Studies of Fe(III), Cu(II), Zn(II), N,N'-Bis(2-hydroxy-1,2-diphenylethanone)ethylenediamine Complexes. *Chemical Methodologies*, **3** (2): 408-424
- Kennedy, I.R. and Hodzic, M. (2021). Partitioning entropy with action mechanics: Predicting chemical reaction rates and gaseous equilibria of reactions of hydrogen from molecular properties. *Entropy*, **23**: 1056-1059.
- Kim, Y.S., Kim, Y.S. and Kim, S.H. (2010). Investigation of Thermodynamic Parameters in the Thermal Decomposition of Plastic Waste-Waste Lube Oil Compounds. *Environmental Science Technology*, **44**: 5313-5317.
- Klippenstein, S. J., Pande, V. S. and Truhlar, D. G. (2014). Chemical kinetics and mechanisms of complex systems: A perspective on recent theoretical advances. *Journal of the American Chemical Society*, **136** (2): 528-546.
- Kulkarni, A. B., Methad, S. N. and Bakale, R. P. (2019). The evaluation of kinetic parameters for cadmium doped Co-Zn ferrite using thermogravimetric analysis. *Ovidius University Annals of Chemistry*, **30**: 60-64.
- Li, D. and Zhong, G. (2014). Synthesis, crystal structure, and thermal decomposition of the cobalt(II) complex with 2-picolinic acid. *The Scientific World Journal*, **11**: 55.
- Linkuviene, V., Talibov, V.O., Danielson, U.H., and Matulis, D. (2018). Introduction of Intrinsic Kinetics of Protein-Ligand Interactions and Their Implications for Drug Design. *J Med Chem* **61**(6), 2292-2302.
- Lyu, R., Huang, Z., Deng, H., Wei, Y., Mou, C. and Wang, L. (2021). Anatomies for the thermal decomposition behaviour and product rule of 5, 5'-dinitro-2 H, 2H'-3, 3'-bi-1, 2, 4-triazole. *RSC Advances*, **11**: 40182-40192.
- Malacaria, L., Corrente, G. A., Beneduci, A., Furia, E., Marino, T. and Mazzone, G. (2021). A review on coordination properties of Al(III) and Fe(III) toward natural antioxidant molecules: Experimental and theoretical insights. *Molecules*, **26**(9): 2603-2610.
- Masoud, M. S., Hemdan, S. S. and Elsamra, R.M. I. (2022). Synthesis, ligating properties, thermal behaviour, computational and biological studies of some azo-transition metal complexes. *Journal of Inorganic and Organometallic Polymers and Materials*, **33** (1): 1-18.
- Masoud, M.S., Ramadan, M. S. and Al-Saify, M.H. (2018). Potentiometric studies and thermodynamic parameters of some pyrimidine compounds and their complexes. *Journal of Pharmaceutical and Analytical Chemistry*, **4**:1-9.
- Ni, Y., Tao, J., Jin, J., Lu, C., Xu, Z., Xu, F., Chen, J. and Kang, Z. (2014). An investigation of the effect of ligands on thermal stability of luminescent samarium complexes. *Journal of Alloys and Compounds*, **612**: 349-354.
- Nikolaev, A. V., Logvinenco, V. A. and Myachina, L. I. (1969). Thermal analysis. *Academic Press, New York, USA*. Pp45
- Ohia, G.N., Amasiatu, G.I. and ajagbe, J.O. (2013). Comprehensive certificate chemistry. 2nd edition. University press Pp 218-219.
- Palmay, P., Mora, M., Barzallo, D. and Bruno, J.C. (2021). Determination of Thermodynamic Parameters of Polylactic Acid by Thermogravimetry under Pyrolysis Conditions. *Journal of Applied Science*, **11**: 10192.
- Papadopoulos, C., Cristóvão, B., Ferenc, W. and Hatzidimitriou, A. G. (2015). Thermoanalytical, magnetic and structural investigation of neutral Co(II) complexes with 2, 2'-dipyridylamine and salicylaldehydes. *Journal of Thermal Analysis and Calorimetry*, **123** (1): 4976-4980.
- Piskulich, Z. A., Mesele, O. O. and Thompson, W. H. (2019). Activation energies and beyond. *The Journal of Physical Chemistry A*, **123** (33): 3967.
- Rodica, O., Badea, M., Marinescu, D. and Calu, L. (2010). Thermal behaviour of some new complexes with bismacrocylic ligands as potential biological active species. *Journal of Thermal Analysis and Calorimetry*, **105** (2): 571-575.
- Sarsenbekova, A. Z., Zhumanazarova, G. M., Tazhbayev, Y. M., Kudaibergen, G. K., Kabieva, S. K., Issina, Z. A., Kaldybayeva, A. K., Mukabylova, A. O. and Kilybay, M. A. (2023). Research the thermal decomposition processes of copolymers based on polypropyleneglycolfumaratephthalate with acrylic acid. *Polymer (Basel)*, **15**(7): 1725-1730.
- Sbirrazzuoli, N. (2020). Determination of pre-exponential factor and reaction mechanism in a model-free way. *Thermochimica Acta*, **691**:178707.
- Sharma, A. K., Tank, P. and Sharma, R. (2017). Thermal behaviour and kinetics of copper (II) soaps and complexes derived from mustard and soyabean oil. *Journal Analytical and Pharmaceutical Res*, **4**(2):14-12.

- Singh, G., Tyagi, V., Singh, P. and Pandey, A. (2020). Estimation of thermodynamic characteristics for comprehensive dairy food processing plant: An energetic and exergetic approach. *Energy*, 194: 116799.
- Sodhi, R. K. and Paul, S. (2019). Metal complexes in medicine: An overview and update from drug design perspective. *Cancer Therapy & Oncology International Journal*, 14 (2): 555883-555890.
- Stroberg, W. and Schnell, S. (2017). On the validity and errors of the pseudo-first order kinetics in ligand-receptor binding. *Mathematical Biosciences*, 287: 3-11.
- Su, H. and Xu, Y. (2018). Application of ITC-based characterization of thermodynamic and kinetic association of ligands with proteins in drug design. *Frontiers in Pharmacology*, 9: 1133-11336.
- Sukarni, S., Prasetyo, A., Sumarli, S., Nauri, I. M. and Permanasari, A. A. (2018). Kinetic analysis of co-combustion of microalgae *spirulina platensis* and synthetic waste through the fitting model. *MATEC Web of Conferences*, 204: 00009.
- Tonbul, Y. and Yurdakoc, K. (2001). Thermogravimetric investigation of the dehydration Kinetics of KSF, K10 and Turkish Bentonite. *Turkish Journal of Chemistry*, 5: 333-339.
- Triyono, T. (2010). Correlation between pre-exponential factor and activation energy of isoamylacohol hydrogenolysis on platinum catalysts. *Indonesian Journal of Chemistry*, 4 (1): 1-5.
- Vafazadeh, R. and Bagheri, M. (2015). Kinetics and mechanism of the ligand exchange reaction between tetradentate Schiff base N, N'-ethylen-bis(salicylalimine) and Ni(N, N'-propylen-bis(salicylalimine)). *South African Journal of Chemistry*, 68: 21-26.
- Valapa, R., Pugazhenthii, G. and Katiyar, V. (2014). Thermal degradation kinetics of sucrose palmitate reinforced poly(lactic acid) biocomposites. *International Journal Biological Macromolecules*, 65: 275-283.
- Vyazovkin, S. (2021). Determining Preexponential factor in model-free kinetic methods: How and Why? *Molecules*, 26(11): 3077.
- Wang, Y., Cao, S. C., Yuan, C., Shi, J., Yang, B. and Dai, Y. (2018). Distinguishing the combustion stage using the preexponential factor and preparation of low-sulfur biomass fuel. *Catalysis Today*, 318: 66-72.
- Wang, Y., Yan, B., Wang Y., Zhang, J., Chen, X. and Bastiaans, R. J. M. (2021). A comparison of combustion properties in biomass-coal blends using characteristic and kinetic analyses. *International Journal of Environmental Research and Public Health*, 18 (24): 12980.
- Zaware, S.K. and Jadhav, S.S. (2015). Kinetic and mechanism of thermal decomposition of binary mixture of ferrous oxalate and copper oxalate in the (1:2) mole ratio. *International Journal of Engineering Research and Technology*, 1(10): 2-11.